Developing a new understanding of the low temperature oxidation of alkanes and implications for low temperature combustion modelling: A case study of *n*-pentane

J. Bugler, S. M. Burke, K. P. Somers, E. J. Silke, H. J. Curran

National University of Ireland, University Road, Galway, Ireland

Corresponding author:

J. Bugler

National University of Ireland Galway

University Road

Galway

Ireland

Email: j.bugler1@nuigalway.ie

Topic: Reaction Kinetics

Number of words (method 1):

Total length (max. 5800):	**5704**
Main text:	2960
Figures and captions: [(∑=329mm+5*10mm)x2.2x1]+176	1010
[(∑=169mm+3*10mm)x2.2x2]+141	1017
References: (39+2)x2.3x7.6	717

Abstract

This study presents a new understanding of low-temperature oxidation kinetics. It is applied to *n*-pentane which is a small alkane, yet has a structure complex enough to allow application of its chemistry to larger molecules. Rate rules for reaction classes important to low-temperature oxidation including those related to the negative temperature coefficient (NTC) region and to first-stage ignition, have been replaced based on recent quantum-chemically derived rate coefficients from the literature [34,35]. Several reaction classes have also been included to allow for the production of types of species detected in low-temperature speciation studies of other *n*-alkanes. Updates to the thermochemistry of the species important in the low-temperature oxidation of hydrocarbons have also been made based on a thorough literature review. A comparison of the model with pressure-time histories from experiments in a rapid compression machine shows a very good agreement for both ignition delay time and pressure rise for both the first and second stage ignition events. The results of this study indicate that major modifications with respect to our understanding of the combustion of straight-chained and branched alkanes are required.

1. Introduction

The low-temperature oxidation of alkanes is of practical importance to the advancement of technologies such as diesel and premixed charge compression ignition (PCCI) engines. Alkanes are the simplest type of hydrocarbon, so knowledge of the combustion of these compounds is essential to the fundamental understanding of the combustion of all hydrocarbons and oxygenated fuels (e.g. alcohols, large methyl esters, etc.). The low-temperature combustion chemistry of *n*-alkanes has been well explored [1–33]. The first low-temperature reaction channels for the oxidation of alkanes were proposed in the late 60's by Knox [6] and Fish [7]. A further improved understanding was published by Pollard [8], Cox and Cole [9] and Walker and Morley [10]. Curran *et al.* successfully applied rate coefficients based on rate estimation rules for the different reaction classes to the autoignition of *n*-heptane [1] and *iso*-octane [33] at low temperature. However, some possible reaction classes were excluded from the low-temperature reaction pathways of these chemical kinetic mechanisms. These involve $\dot{O}_2QOOH$ species undergoing reactions similar to those included for $R\dot{O}_2$ and $\dot{Q}OOH$ species, leading to the formation of products other than carbonyl-hydroperoxides. Silke [3] and Glaude *et al*. [10] have performed in-depth studies of some of these "alternative" reaction classes for the low-temperature oxidation of *n*-heptane. A simplified scheme for the primary oxidation reactions of alkanes, including these "alternative" reaction classes is shown in Fig. 1 (Ṙ, Q̇ and U̇ represent alkyl species C_nH_{2n+1}, C_nH_{2n} and C_nH_{2n-1}, respectively). "Alternative" isomerisations of $\dot{O}_2QOOH$, and cyclic ether formation from $\dot{O}_2QOOH$ species were included to Silke's *n*-heptane mechanism. Examples of these types of reactions for *n*-pentane can be seen in Fig. 2. By assigning rate coefficients based on the rate rules of Curran *et al*. [1], Silke [3] showed that the addition of these reaction classes resulted in large changes to numerically derived ignition delay times, with the addition of some resulting in predicted ignition delay times being orders of magnitude faster than

those recorded in the experiments (see Figures 3). It would appear that the rate rules being used at the time were not suitable for application to these alternative reactions.

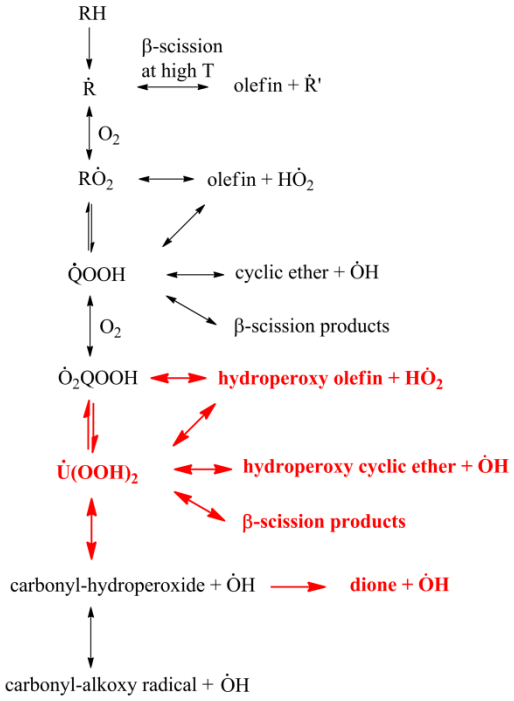

Figure 1: Lumped kinetic scheme of the primary oxidation reactions (species and arrows in highlighted in red represent pathways not previously considered for *n*-pentane)

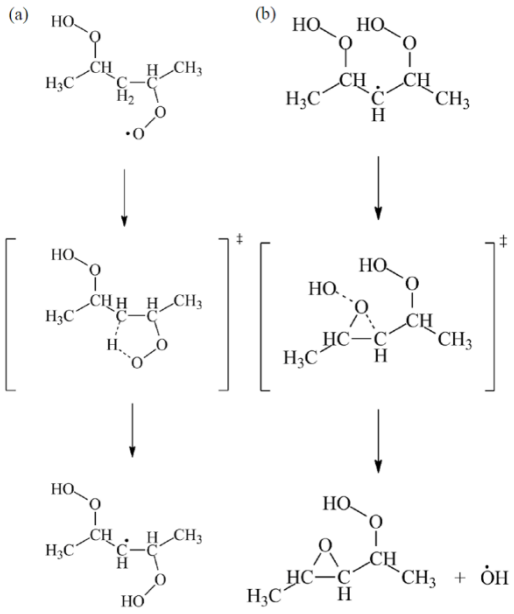

Figure 2: Examples of reaction classes previously added to Silke [3] *n*-heptane mechanism (a) "Alternative" isomerisation of Ȯ2QOOH. (b) Hydroperoxy cyclic ether formation from Ȯ2QOOH.

It is essential that all pathways are investigated in order to gain a detailed understanding of a fuel's behaviour. The fact that the rate rules of Curran *et al.* [1] were not suitable for application to the alternative pathways, yet the predictions of the *n*-heptane and *iso*-octane models reproduced data very well, points to a fundamental lack of knowledge in some aspect of the modelling. Since then, a thorough literature review [39] of thermochemical properties was undertaken for C_1–C_4 alkanes, alkenes, alcohols, hydroperoxides and alcoholic hydroperoxides and their associated radicals from a variety of sources, including high level *ab-initio* studies, experimental studies, online databases, and review studies leading to an update of the THERM [40] group values. They were then used to update the existing thermochemistry parameters of the following classes of C_5 species: fuel (RH), fuel radicals (Ṙ), olefins, alkyl hydroperoxides (RO_2H), alkyl peroxy radicals ($R\dot{O}_2$), hydroperoxy alkyl radicals (ṠOOH), cyclic ethers, hydroperoxy alkyl peroxy radicals ($\dot{O}_2$QOOH) and carbonyl-hydroperoxides. These are provided as Supplementary Material.

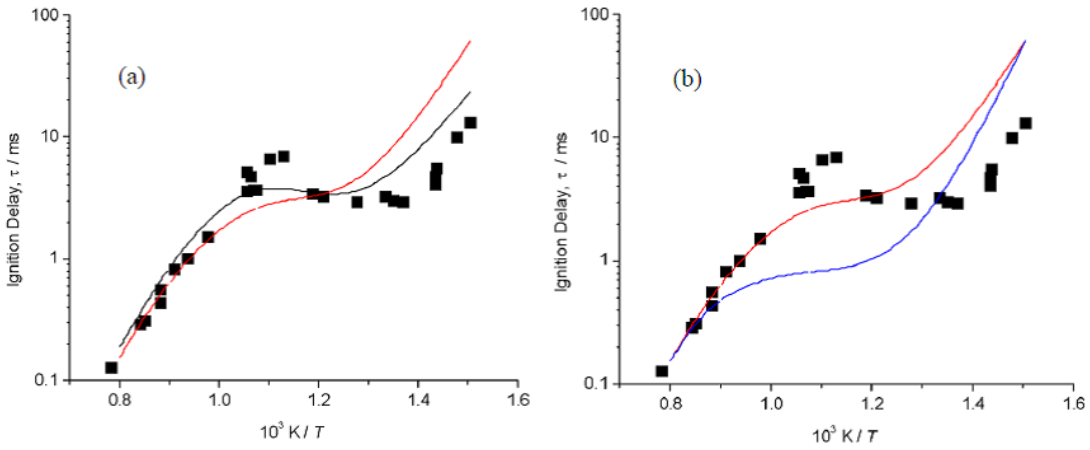

Figure 3: Effect of (a) "alternative" isomerisations of $\dot{O}_2$QOOH and (b) hydroperoxy cyclic ether formation from $\dot{U}(OOH)_2$ for *n*-heptane, Φ = 1.0 in 'air', ~13.5 atm [3]. ■ Ciezki *et al.* [38]; — Model of Curran *et al*; — Model including "alternative" isomerisations; — Model including hydroperoxy cyclic ether formation.

The inclusion of the updated thermochemistry lead to a significant increase in numerically derived ignition delay times (Fig. 4). This is due a change in the equilibrium coefficients of the reactions involving the updated species. These results show that with our now better understanding of the thermochemistry of species relevant to low-temperature combustion, a major overhaul of the rate coefficients of reactions important in the low-temperature regime is necessary.

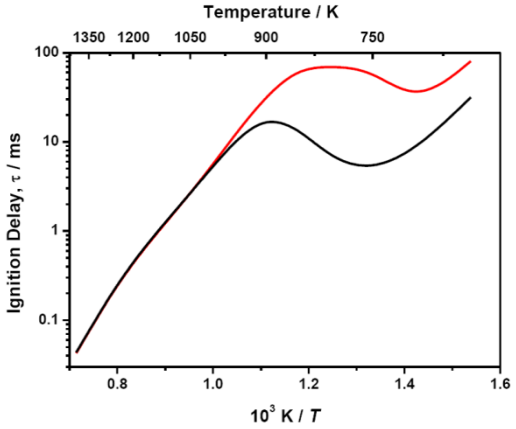

Figure 3: Effect of updated thermochemistry. *n*-pentane, Φ = 1.0 in 'air', 10 atm. — Model predictions using old thermochemistry; — Model predictions using new thermochemistry.

Since the work of Curran *et al*. [1,33], computational chemistry has improved significantly. Villano *et al.* have performed systematic calculations of rate coefficients for reactions important to the low-temperature oxidation of alkanes, using the CBS-QB3 method [29,30]. Recently, Karwat *et al.* [26] studied the oxidation of *n*-heptane in a rapid compression facility and demonstrated success in using the Villano *et al.* data.

Here we apply the same rate rules to *n*-pentane but also carry out a more complete analysis, allowing for the possibility of new reaction classes, to test whether or not these are important to the low temperature oxidation of *n*-pentane.

n-Pentane was chosen as a case study for application of these new rate rules because of its relatively small size, but also because it is the first normal alkane with a chain long enough between its two outermost secondary carbons to allow for facile progression towards chain branching reactions

through 6-membered transition state rings, which have a low ring-strain energy. For these reasons, *n*-pentane serves as a good test for application of *n*-alkane low-temperature reaction class rate rules to larger normal alkanes.

2. Experimental

2.1 Rapid Compression Machine

Ignition delay times were measured using a clone of a twin opposed-piston rapid compression machine originally developed by Affleck and Thomas at Shell-Thornton [31] and re-commissioned at NUIG in the late 1990s [32,33]. Non-reactive experiments were performed in which oxygen was replaced by nitrogen in a mixture, in order to obtain pressure-time histories which are converted to volume-time histories to be used in chemical kinetic simulations to simulate the effects of compression and heat loss. Details of the facility and experimental procedures are given in previous publications [16,22].

3. Chemical Kinetic Modelling

The mechanism presented in *this work* supersedes that of Healy *et al.* [5], the rate rules of which were based on the work of Curran *et al.* [1]. A thorough literature review [34] of thermochemical properties was undertaken for C_1–C_4 alkanes, alkenes, alcohols, hydroperoxides and alcoholic hydroperoxides and their associated radicals from a variety of sources, including high level ab initio studies, experimental studies, online databases, and review studies leading to an update of the THERM [35] group values. They were then used to update the existing thermochemistry parameters of the following classes of C_5 species: fuel (RH), fuel radicals (Ṙ), olefins, alkyl hydroperoxides (RO_2H), alkyl peroxy radicals ($R\dot{O}_2$), hydroperoxy alkyl radicals ($\dot{Q}OOH$), cyclic ethers, hydroperoxy alkyl peroxy radicals ($\dot{O}_2QOOH$) and carbonyl-hydroperoxides.

The thermochemistry values used for 2-methyltetrahydrofuran (the cyclic ether produced in the highest abundance from the low temperature oxidation of *n*-pentane) come from the work by Simmie [36]. The enthalpy and entropy values calculated by Simmie are within < ±0.5% at 298 K of the values attained when using the updated thermochemistry group values.

Moreover, many changes have been made to the rate coefficients in the mechanism, and several new reaction classes have been added. Effort has also been made to make every reaction reversible; for example, carbonyl-hydroperoxide → Ṙ + R=O + ȮH, which proceeds via a β-scission followed by another β-scission is now treated as two elementary reaction steps (1. carbonyl-hydroperoxide ↔ carbonyl-alkoxy radical + ȮH, 2. carbonyl-alkoxy radical ↔ Ṙ + R=O), and each step is assigned an elementary rate coefficient.

3.1 Updated Reaction Classes

Changes were made to the following reaction classes:

O_2 addition to fuel radical ($\dot{R} + O_2 \leftrightarrow R\dot{O}_2$)

The rate coefficients used for O_2 addition to the fuel radical are taken from Miyoshi [37] who used variational transition state theory and RRKM theory/master equation calculations for archetypal alkyl radical + O_2 systems.

The rate coefficients for the following classes of reactions were taken from the work of Villano *et al.* [29].

- *Concerted elimination of $H\dot{O}_2$ from alkyl peroxy radical ($R\dot{O}_2 \leftrightarrow$ olefin + $H\dot{O}_2$)*
- *Isomerisation of alkyl peroxy radical to hydroperoxy alkyl radical ($R\dot{O}_2 \rightleftharpoons \dot{Q}OOH$)*

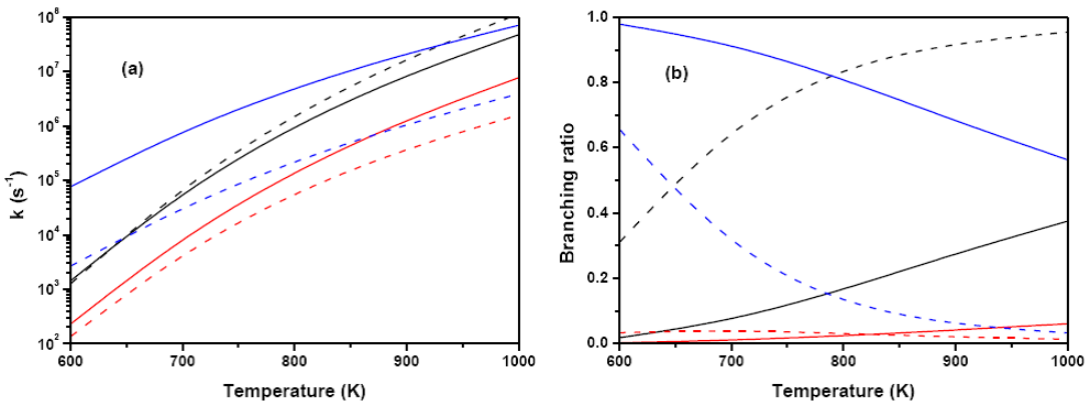

Figure 3: Comparison of (a) total rate coefficients and (b) branching ratios of pathways of RO_2. Solid lines: Old rate coefficients/branching ratios. Dashed lines: Updated rate coefficients/branching ratios. — $R\dot{O}_2 \leftrightarrow \dot{R} + O_2$; — $R\dot{O}_2 \leftrightarrow$ olefin + $H\dot{O}_2$; — $R\dot{O}_2 \rightleftharpoons \dot{Q}OOH$.

Figure 3 shows a comparison of the total rate coefficients, and of the branching ratios of the reaction pathways of the alkyl peroxy radical from 600–1000 K. Figure 3 (a) shows that the greatest change between the old and updated rate coefficients is the increase of the total rate coefficient for isomerisation of alkyl peroxy radical to give hydroperoxy alkyl radical, which has increased by over an order of magnitude. Figure 3 (b) shows a significant shift in the branching ratios of the reaction pathways of the alkyl peroxy radical. Using the old rate rules resulted in the dissociation of the alkyl

peroxy radical to give alkyl radical and O_2 being the dominant pathway above 650 K. The major change shown here is the dominance of the isomerisation pathway of alkyl peroxy radicals to produce hydroperoxy alkyl radicals at temperatures between 600 and 1000 K using the updated rate coefficients. The decrease of the total rate coefficient for $R\dot{O}_2$ dissociation coupled with the significant increase in the total rate coefficient for $R\dot{O}_2 \rightleftharpoons \dot{Q}OOH$ isomerisations (which can subsequently go on to react with O_2 and lead to chain branching) leads to a significant predicted increase in reactivity.

The rate coefficients for the following classes of reactions were taken from a second paper by Villano *et al.* [30] in which rate coefficients are given for reaction classes important to the hydroperoxy alkyl radical.

- *β-scission of hydroperoxy alkyl radical to give an olefin + $H\dot{O}_2$ ($\dot{Q}OOH \leftrightarrow$ olefin + $H\dot{O}_2$)*
- *Cyclic ether formation ($\dot{Q}OOH \leftrightarrow$ cyclic ether + $\dot{O}H$)*
- *β-scission of hydroperoxy alkyl radical to give other products ($\dot{Q}OOH \leftrightarrow$ β-scission products)*

O_2 addition to hydroperoxy alkyl radical ($\dot{Q}OOH + O_2 \leftrightarrow \dot{O}_2QOOH$)

The rate coefficients used for these reactions are based on those used for O_2 addition to the fuel radical, with the A-factor reduced by 45%. This reduction of $\dot{Q}OOH + O_2$ relative to $\dot{R} + O_2$ is in general agreement with the results of Franklin Goldsmith *et al.* [4] and Asatryan and Bozzelli [25] who found that the second O_2 addition reaction is typically slower than the first by approximately a factor of 2.

3.2 New Reaction Classes

The classes of reactions described hereafter have been added to the original mechanism. Some of these classes have been previously considered by Silke for *n*-heptane oxidation [3], but, as will be shown, resulted in deterioration of numerically derived ignition delay time results when compared to the previous mechanism [1].

Concerted elimination of $H\dot{O}_2$ from hydroperoxy alkyl peroxy radical ($\dot{O}_2QOOH \leftrightarrow$ hydroperoxy olefin + $H\dot{O}_2$)

This reaction class has not previously been considered [1,3,5], and is analogous to the concerted elimination reactions of the alkyl peroxy radical and we adopt the same rate coefficients.

Isomerisation of hydroperoxy alkyl peroxy radical to di-hydroperoxy alkyl radical ($\dot{O}_2QOOH \rightleftharpoons \dot{U}(OOH)_2$)

This reaction class was also not previously considered in *n*-pentane oxidation schemes [5], but was included *n*-heptane mechanisms by Silke [3] and Glaude [10]. The rate coefficients used for these reactions in *this work* are based on analogous isomerisations of alkyl peroxy radical to give hydroperoxy alkyl radical. If the hydrogen being abstracted is bound to a carbon, which is bound to a hydroperoxy group, the activation energy has been reduced by 3 kcal mol^{-1}, as recommended by Curran *et al.* [1], as well as the A-factor being adjusted according to the number of hydrogen atoms available for abstraction. Comparisons of the effect of this reaction class on numerically derived ignition delay times of the Silke model versus that of the model presented in *this work* are shown in Fig. 4.

β-scission of di-hydroperoxy alkyl radical to give hydroperoxy olefin + $H\dot{O}_2$ ($\dot{U}(OOH)_2 \leftrightarrow$ hydroperoxy olefin + $H\dot{O}_2$)

Another reaction class previously not considered for *n*-pentane, these reactions are analogous to those of the hydroperoxy alkyl radical undergoing β-scission to give olefin + $H\dot{O}_2$ and we adopt the same rate coefficients [30].

Hydroperoxy cyclic ether formation ($\dot{U}(OOH)_2 \leftrightarrow$ hydroperoxy cyclic ether + $\dot{O}H$)

This reaction class was previously added to the *n*-heptane mechanism of Silke [3], and was shown to have a significant effect on numerically derived ignition delay times (Fig. 5 (a)). Although the addition of this reaction class to the *n*-pentane mechanism resulted in a reduction of numerically derived ignition delay times (Fig. 5 (b)), it is not nearly as pronounced an effect as was seen for *n*-heptane predictions. Rate coefficients for these reactions are based on analogous reactions of the hydroperoxy alkyl radical to form cyclic ethers.

β-scission of di-hydroperoxy alkyl radical to give other products ($\dot{U}(OOH)_2 \leftrightarrow$ β-scission products)

Rate coefficients for these reactions are based on analogous β-scission reactions of the hydroperoxy alkyl radical to give other, minor products [30].

β-scission of di-hydroperoxy alkyl radical to give carbonyl-hydroperoxide + $\dot{O}H$ ($\dot{U}(OOH)_2 \leftrightarrow$ carbonyl-hydroperoxide + $\dot{O}H$)

These reactions involve the β-scission of the O–O bond of the hydroperoxy group, which is bound to a carbon radical. These reactions occur very quickly, and so an equilibrium effectively does not take place between the preceding $\dot{O}_2QOOH$ and $\dot{U}(OOH)_2$ species.

H atom abstraction from carbonyl-hydroperoxide to give dione + $\dot{O}H$ (carbonyl-hydroperoxide + $\dot{R} \rightarrow$ dione + $\dot{O}H$ + RH)

Considering the work of Battin-Leclerc *et al.* [19] and Herbinet *et al.* [2,21] on the low-temperature oxidation of *n*-butane and *n*-heptane suggests that diones are formed from the low-temperature oxidation of *n*-alkanes. The formation of 1,3- and 2,4-pentadione as a result of hydrogen atom

abstraction at the site adjacent to the hydroperoxy group has been considered. Herbinet *et al.* [2] proposed that the formation of diones from carbonyl-hydroperoxides is mainly due to β-scission of the C–H bond adjacent to the hydroperoxy group once the O–O bond of the hydroperoxy group fissions. Elimination of water from the carbonyl-hydroperoxides to form diones is also considered in their work. However, if diones are mainly formed from the β-scission reaction of carbonyl-alkoxy radicals, one would expect to see more diones produced from the oxidation of branched alkanes, as β-scissions of the weaker C–C bonds would occur. A study of the low temperature oxidation of the isomers of hexane found that diones were only formed from the *n*- isomer []. This would suggest that their formation could be as a result of hydrogen atom abstraction from carbonyl-hydroperoxides and this is the mechanism proposed here for dione formation.

Decomposition of carbonyl-alkoxy radical

The carbonyl-alkoxy radical decomposes via β-scission of a C–C bond. Herbinet *et al.* [2] calculated rate coefficients for these β-scissions for a 2,4-pentyl carbonyl-alkoxy radical using the CBS-QB3 method. Although their work focused on *n*-heptane oxidation, an *n*-pentane analogy was used in order to reduce CPU time. Their rate coefficients were used for the reactions in this class.

4. Results and discussion

RCM experiments were simulated using the closed homogeneous batch reactor module in CHEMKIN-Pro [39]. For the simulation of RCM experiments, the calculations use volume profiles generated from non-reactive pressure traces. The volume history is used to simulate reaction during the compression stroke, and the heat losses that occur during the experiments.

Figure 6 shows a comparison of model simulations with experimental pressure-time histories from the RCM. There is excellent agreement between the model and experiment for these cases. First and second stage ignition delay times are well reproduced by the model. Moreover, the pressure rise due to first-stage ignition is well captured. The pressure immediately after the first-stage ignition in the

experimental data is approximately 90% of that predicted by the model across the temperature range in which first-stage ignition is observed.

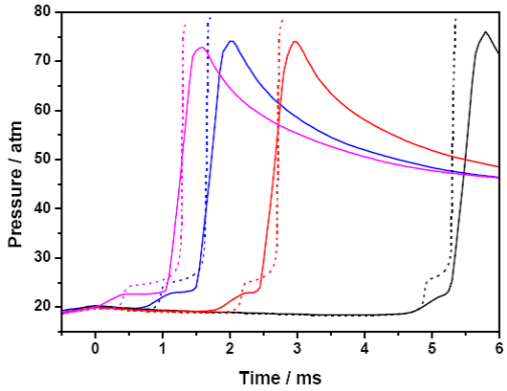

Figure 6: Comparison of experimental and simulated pressure time histories. Φ = 1.0 in 'air'. Diluent = 100% N_2. Solid lines represent experiments. Dashed lines represent simulations (using volume history from RCM): p_C = 20 atm, T_C = 718–774 K.

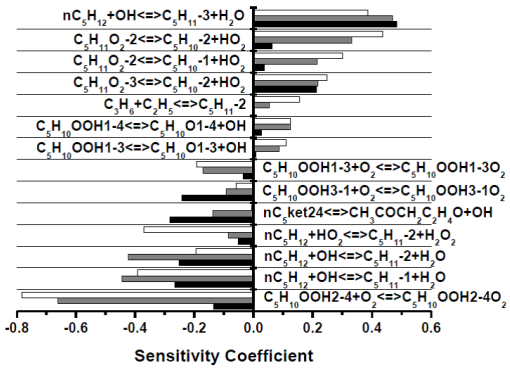

Figure 7: Ignition delay sensitivity analysis. Φ = 1.0 in 'air', *p* = 10 atm, T = 650 K (black bars), 750 K (grey bars) and 850 K (open bars). Positive coefficients correspond to reactions which increase ignition delay time and vice versa.

Figure 7 shows sensitivity analyses from 650–850 K for Φ = 1.0 in 'air', at 10 atm. For brevity, only C_5 species are shown. It can be seen that hydrogen atom abstractions from the fuel by hydroxyl radical are very important and have a significant effect on ignition delay time predictions depending on the site from which abstraction occurs. Abstraction from the 1- and 2- sites on *n*-pentane by ȮH radical promote reactivity because the primary consumption pathway for the alkyl radicals is the

addition of O_2 to produce alkyl peroxy radicals, which isomerise to form ȮOOH, and can continue on to pathways leading to chain branching. Conversely, abstraction from the 3- site (central carbon) is inhibiting. Even though the main reaction pathway for the resulting alkyl radical is O_2 addition, the alkyl peroxy radical that is formed mainly goes to 2-pentene and hydroperoxy radical (i.e. the propagating channel dominates over pathways which can lead to chain branching). Reactions of O_2 addition to ȮOOH are shown to decrease ignition delay time. This is because they can take part in reactions leading to chain branching reactions. Propagating reactions such as concerted elimination of $HȮ_2$ radical from $RȮ_2$, and ȮOOH going on to form cyclic ethers and ȮH radical are shown to increase ignition delay time.

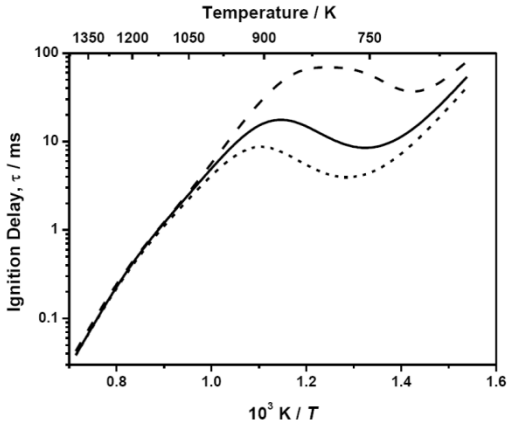

Figure 8: Effect of updates to thermochemistry and rate coefficients. Solid line = updates to both thermochemistry and rate coefficients. Dashed line = updates to thermochemistry only. Dotted line = updates to rate coefficients only. All simulations shown are at constant volume conditions.

Figure 8 shows the effect of updates to the thermochemistry alone, and updates to the rate coefficients alone on numerically derived ignition delay times, alongside the current model in which both have been updated. It is shown that updating one without updating the other has a significant effect, and ultimately results in deterioration of model predictions, especially in the low temperature regime. This highlights the importance of taking a careful and consistent approach to compiling thermochemical and kinetic data when building a chemical kinetic model.

5. Conclusions

This study presents a major update to the understanding of the low temperature oxidation of *n*-pentane with respect to the both the thermochemical and kinetic estimations used therein.

There have been significant changes to the rate coefficients for the reaction classes important to low temperature oxidation, including those related to the NTC region and first stage ignition. By using the most up-to-date thermochemistry group values and rate coefficients from several recent publications [2,29,30,34,36,37], the current model shows very good agreement to experimental data. It was found that changes to both the thermochemistry and the mechanism were required in order to replicate experiments so well. Updates to the thermochemistry alone resulted in numerically derived ignition delay times being grossly overestimated when compared to experimental data. Conversely, updates to the rate coefficients alone resulted in numerically derived ignition delay times being far too short.

Past models [1,5,22,28] that used rate rule estimates for reaction classes replicated experimental data very well. However, it would seem that this is due to a series of compensating errors in terms of both thermochemistry and rate coefficient assignments, which may have been overcome in certain instances by not allowing thermochemical equilibrium to hold (i.e. by definition of rate coefficients in both the forward and reverse directions).

This work represents a major change to the understanding of the low temperature combustion of alkanes, and shows that careful consideration of both thermochemistry and rate coefficients in a consistent manner is essential in order to improve this understanding.

Additional reaction classes (some of which were previously explored but ultimately resulted in numerically derived ignition delay time predictions deteriorating overall, for *n*-heptane) have been included and have not had such a large effect on model predictions as that which was previously seen

[3]. The reason for this may be a result of more accurate thermochemistry values and more accurate rate coefficients than those that were previously used. It is important that these reaction pathways are included in alkane (and other fuel types) reaction mechanisms, as detailed chemistry gives a precise picture of *all* the reactions controlling the various stages of combustion, and is imperative for a detailed understanding of various fuel behaviour and model predictions in a multitude of combustion systems.

Future work would entail applying the thermochemistry, rate coefficients and pathways used in *this work* to larger straight-chained and branched alkanes.

Acknowledgements

The authors would like to thank Dr. Charles K. Westbrook, Dr. William J. Pitz and Dr. Marco Mehl from LLNL, and Dr. S. Mani Sarathy from KAUST, for helpful discussions.

References

[1] H. J. Curran, P. Gaffuri, W. J. Pitz, C. K. Westbrook, Combust. Flame 114 (1–2) (1998) 149–177.

[2] O. Herbinet, B. Husson, Z. Serinyel, M. Cord, V. Warth, R. Fournet, P. A. Glaude, B. Sirjean, F. Battin-Leclerc, Z. Wang, M. Xie, Z. Cheng, F. Qi, Combust. Flame 159 (12) (2012) 3455–3471.

[3] E. J. Silke, *The Influence of Fuel Structure on Combustion as Demonstrated by the Isomers of Heptane: a Rapid Compression Machine Study & Detailed Kinetic Modelling of n-Heptane*, PhD thesis, School of Chemistry, NUI Galway, 2005.

[4] C. Franklin Goldsmith, W. H. Green, S. J. Klippenstein, J. Phys. Chem. A 116 (13) (2012) 3325–3346.

[5] D. Healy, D. M. Kalitan, C. J. Aul, E. L. Petersen, G. Bourque, H. J. Curran, Energy & Fuels 24 (3) (2010) 1521–1528.

[6] J. H. Knox, In: P. G. Ashmore, T. M. Sugden, F. S. Dainton, (Eds.), Photochemistry and reaction kinetics, Cambridge: Cambridge University Press; 1967.

[7] A. Fish, Oxidation of organic compounds, vol. 2. Adv. Chem. Ser. 1968; 76: 69.

[8] R. T. Pollard, Hydrocarbons, In: C. H. Bamford, C. F. H. Tipper, (Eds.), Comprehensive chemical kinetics: gas-phase combustion, vol. 17. Amsterdam: Elsevier; 1977.

[9] R. A. Cox, J. A. Cole, Combust. Flame 60 (1985) 109–123.

[10] R. W. Walker, C. Morley, Basic chemistry of combustion, In: M. J. Pilling, (Ed.), Comprehensive chemical kinetics: low-temperature combustion and autoignition, vol. 35. Amsterdam: Elsevier; 1997.

[11] J. F. Griffiths, P. A. Halford-Maw, D. J. Rose, Combust. Flame 95 (3) (1993) 291–306.

[12] R. Minetti, M. Carlier, M. Ribaucour, E. Therssen, L. R. Sochet, Combust. Flame 102 (3) (1995) 298–309.

[13] K. A. Sahetchian, R. Rigny, S Circan, Combust. Flame 85 (3–4) (1991) 511–514.

[14] E. Ranzi, P. Gaffuri, T. Faravelli, P. Dagaut, Combust. Flame 103 (1–2) (1995) 91–106.

[15] P. A. Glaude, F. Battin-Leclerc, R. Fournet, V. Warth, G. M. Côme, G. Scacchi, Combust. Flame 122 (4) (2000) 451–462.

[16] P. A. Glaude, V. Conraud, R. Fournet, F. Battin-Leclerc, G. M. Côme, G. Scacchi, P. Dagaut, M. Cathonnet, Energy & Fuels 16 (5) (2002) 1186–1195.

[17] W. Su, H. Huang, Fuel 84 (9) (2005) 1029–1040.

[18] J. D. DeSain, S. J. Klippenstein, J. A. Miller, C. A. Taatjes, J. Phys. Chem. A 107 (22) (2003) 4415–4427.

[19] J. C. Rienstra-Kiracofe, W. D. Allen, H. F. Schaefer, J. Phys. Chem. A 104 (44) (2000) 9823–9840.

[20] J. D. DeSain, C. A. Taatjes, J. A. Miller, S. J. Klippenstein, D. K. Hahn, Faraday Discuss. 119 (2002) 101–120.

[21] D. Healy, N. S. Donato, C. J. Aul, E. L. Petersen, C. M. Zinner, G. Bourque, H. J. Curran, Combust. Flame 157 (8) (2010) 1526–1539.

[22] G. Bourque, D. Healy, H. J. Curran, C. M. Zinner, D. M. Kalitan, J. de Vries, C. J. Aul, E. L. Petersen, J. Eng. Gas Turbines Power 132 (2) (2009) 21504–21515.

[23] A. Jalan, I. M. Alecu, R. Meana-Paneda, J. Aguilera-Iparraguire, K. R. Yang, S. S. Merchant, D. G. Truhlar, W. H. Green, J. Am. Chem. Soc. 135 (2013) 11100–11114.

[24] F. Battin-Leclerc, O. Herbinet, P. A. Glaude, R. Fournet, Z. Zhou, L. Deng, H. Guo, M. Xie, F. Qi, Proc. Combust. Inst. 33 (2011) 325–331.

[25] J. A. Miller, S. J. Klippenstein, S. H. Robertson, Proc. Combust. Inst. 28 (2000) 1479–1486.

[26] O. Herbinet, F. Battin-Leclerc, S. Bax, H. Le Gall, P. A. Glaude, R. Fournet, Z. Zhou, L. Deng, H. Guo, M. Xie, F. Qi, Phys. Chem. Chem. Phys. (13) (2011) 296–308.

[27] S. M. Gallagher, H. J. Curran, W. K. Metcalfe, D. Healy, J. M. Simmie, G. Bourque, Combust. Flame 153 (1–2) (2008) 316–333.

[28] H. -H. Carstensen, A. M. Dean, Proc. Combust. Inst. 30 (2005) 995–1003.

[29] H. -H. Carstensen, A. M. Dean, O. Deutschmann, Proc. Combust. Inst. 31 (2007) 149–157.

[30] R. Asatryan, J. W. Bozzelli, J. Phys. Chem. A 114 (29) (2010) 7693–7708.

[31] D. M. A. Karwat, S. W. Wagnon, M. S. Wooldridge, C. K. Westbrook, Combust. Flame 160 (12) (2013) 2693–2706.

[32] C. K. Westbrook, H. J. Curran, W. J. Pitz, J. F. Griffiths, C. Mohamed, S. K. Wo, Symposium (International) on Combustion 27 (1998) 371–378.

[33] H. J. Curran, P. Gaffuri, W. J. Pitz, C. K. Westbrook, Combust. Flame 129 (3) (2002) 253–280.

[34] S. M. Villano, L. K. Huynh, H. -H. Carstensen, A. M. Dean, J. Phys. Chem. A 115 (46) (2011) 13425–13442.

[35] S. M. Villano, L. K. Huynh, H. -H. Carstensen, A. M. Dean, J. Phys. Chem. A 116 (21) (2012) 5068–5089.

[36] W. S. Affleck, A. Thomas, Proc. Inst. Mech. Eng. 183 (1968) 365–385.

[37] L. Brett, *Re-commissioning of a rapid compression machine and computer modelling of hydrogen and methane autoignition*, PhD thesis, School of Chemistry, NUI Galway 1999.

[38] L. Brett, J. MacNamara, P. Musch, J. M. Simmie, Combust. Flame 124 (1–2) (2001) 326–329.

[39] S. M. Burke, *Development of a Chemical Kinetic Mechanism for Small Hydrocarbons*, PhD thesis, School of Chemistry, NUI Galway 2014.

[40] E. R. Ritter, J. W. Bozzelli, Int. J. Chem. Kin. 23 (9) (1991) 767–778.

[41] J. M. Simmie, J. Phys. Chem. A, 116 (18) (2012) 4528–4538.

[42] A. Miyoshi, Int. J. Chem. Kin. 44 (1) (2012) 59–74.

[43] H. K. Ciezki, G. Adomeit, Combust. Flame 93 (4) (1993) 421–433.

[44] CHEMKIN-PRO 15101, Reaction Design, San Diego, 2010.